THE JOURNAL OF BIOLOGICAL CHEMISTRY VOL. 284, NO. 52, pp. 36387–36394, December 25, 2009

Transient Receptor Potential Canonical Type 1 (TRPC1) Operates as a Sarcoplasmic Reticulum Calcium Leak Channel in Skeletal Muscle*

Received for publication, October 6, 2009 Published, JBC Papers in Press, October 29, 2009, DOI 10.1074/jbc.M109.073221

Céline Berbey, Norbert Weiss, Claude Legrand, and Bruno Allard[1]

From the Laboratoire de Physiologie Intégrative, Cellulaire, et Moléculaire, Université de Lyon, Université Lyon 1, CNRS Unité Mixte de Recherche 5123, 69622 Villeurbanne Cedex, France

Extensive studies performed in nonexcitable cells and expression systems have shown that type 1 transient receptor potential canonical (TRPC1) channels operate mainly in plasma membranes and open through phospholipase C-dependent processes, membrane stretch, or depletion of Ca^{2+} stores. In skeletal muscle, it is proposed that TRPC1 channels are involved in plasmalemmal Ca^{2+} influx and stimulated by store depletion or membrane stretch, but direct evidence for TRPC1 sarcolemmal channel activity is not available. We investigated here the functional role of TRPC1 using an overexpressing strategy in adult mouse muscle fibers. Immunostaining for endogenous TRPC1 revealed a striated expression pattern that matched sarcoplasmic reticulum (SR) Ca^{2+} pump immunolabeling. In cells expressing TRPC1-yellow fluorescent protein (YFP), the same pattern of expression was observed, compatible with a longitudinal SR localization. Resting electric properties, action potentials, and resting divalent cation influx were not altered in TRPC1-YFP-positive cells. Poisoning with the SR Ca^{2+} pump blocker cyclopiazonic acid elicited a contracture of the fiber at the level of the overexpression site in presence and absence of external Ca^{2+} which was not observed in control cells. Ca^{2+} measurements indicated that resting Ca^{2+} and the rate of Ca^{2+} increase induced by cyclopiazonic acid were higher in the TRPC1-YFP-positive zone than in the TRPC1-YFP-negative zone and control cells. Ca^{2+} transients evoked by 200-ms voltage clamp pulses decayed slower in TRPC1-YFP-positive cells. In contrast to previous hypotheses, these data demonstrate that TRPC1 operates as a SR Ca^{2+} leak channel in skeletal muscle.

Transient receptor potential canonical 1 (TRPC1)[2] proteins consist of nonselective cation channels expressed in a great variety of multicellular organisms (1, 2). Extensive studies performed in nonexcitable cells or involving heterologously expressed channels have shown that TRPC1 channels operate mainly in homo- or heteromeric association with other TRPC isoforms as Ca^{2+}-permeable channels in the plasma membrane. Parameters that control TRPC1 channel opening remain controversial. TRPC1 channels could be activated by direct interaction with endoplasmic reticulum inositol trisphosphate receptors or at least through phospholipase C-dependent processes, membrane stretch, or depletion of intracellular Ca^{2+} stores (3). Much less data are available concerning endogenous TRPC1 channels in excitable cells. In skeletal muscle, TRPC1 proteins were first shown to be expressed in the sarcolemma of muscles from dystrophin-deficient mouse (*mdx*), a murine model of Duchenne muscular dystrophy, and were proposed to mediate a sarcolemmal store-operated Ca^{2+} influx in adult fibers (4) and contribute to cell migration and fusion in cultured myoblasts as store-operated or stretch-activated channels (5, 6). Gervásio *et al.* (7) confirmed the sarcolemmal localization of TRPC1 in mouse muscle and indicated that the sarcolemmal level of TRPC1 was slightly increased in *mdx* fibers. Stiber *et al.* (8) also described a sarcolemmal pattern of expression associated with a striated transversal pattern assumed to correspond to costamers at the level of Z discs. TRPC1 was also found to associate with skeletal muscle scaffolding proteins, including caveolin-3 and Homer1 in adult muscle fibers and dystrophin and α1-syntrophin in cultured myotubes (7–9).

Taken together, these data suggest that skeletal muscle TRPC1 channels are involved in sarcolemmal Ca^{2+} influx possibly stimulated by store depletion or membrane stretch, but direct evidence for the existence of a measurable Ca^{2+} conductance supported by TRPC1 channels at resting potentials is not available. We previously showed in adult mouse muscle fibers that sarcoplasmic reticulum (SR) Ca^{2+} depletion failed to induce any increase in the resting whole-cell conductance and inward single channel activity (10). We also demonstrated that the resting and store-operated Ca^{2+} entries detected by the Mn^{2+} quenching method did not produce any measurable macroscopic current in adult muscle cells (11). If TRPC1 is actually involved in Ca^{2+} influx, our results suggest that the ion current generated by TRPC1 activity is too minute to be resolved, or, alternatively, that TRPC1 channel is not active in the plasma membrane and indirectly influences plasmalemmal Ca^{2+} influx. In the present study, we demonstrate that TRPC1 channels are expressed in the SR membrane of adult skeletal muscle cells, and, using an overexpression strategy, we report that TRPC1 operates as a SR Ca^{2+} leak channel.

* This work was supported by grants from the Université Lyon 1, the Centre National de la Recherche Scientifique, the Association Française contre les Myopathies, and the Agence Nationale de la Recherche.

[1] To whom correspondence should be addressed: Université de Lyon, Université Lyon 1, CNRS UMR 5123, Laboratoire de Physiologie Intégrative, Cellulaire et Moléculaire, 43 bd du 11 novembre 1918, 69622 Villeurbanne cedex, France. Tel.: 33-4-72-43-10-32; Fax: 33-4-72-44-79-37; E-mail: bruno.allard@univ-lyon1.fr.

[2] The abbreviations used are: TRPC, transient receptor potential canonical; AP, action potential; CPA, cyclopiazonic acid; di-8-ANEPPs, pyridinium, 4-[2-[6-(dioctylamino)-2-naphthalenyl]ethenyl]-1-(3-sulfopropyl)-, inner salt; SERCA-1, sarco(endo)plasmic reticulum Ca^{2+} ATPase-1; SR, sarcoplasmic reticulum; YFP, yellow fluorescent protein.

EXPERIMENTAL PROCEDURES

Plasmid Preparation—The human TRPC1 cDNA (into pcDNA3.1, kindly provided by Craig Montell) was generated by amplifying the TRPC1 sequence using standard PCR. The product was subcloned in-frame within the KpnI-Age I sites of the polylinker of the enhanced YFP-encoding vector (pEYFP-N1; Clontech) so that the expressed fusion proteins were C-terminally tagged with yellow fluorescent protein (YFP).

In Vivo Transfection of Interosseal Muscles in Adult Mice—All experiments were performed using 3–10-week-old male OF1 mice in accordance with the guidelines of the French Ministry of Agriculture (87/848) and of the European Community (86/609/EEC). Plasmid DNA (about 50 μl at 10 μg/μl) was injected into the footpads of the animal at different locations. Following injection, the foot was placed between two electrodes linked to an electroporator (BTX ECM 830), and eight pulses of 200 V/cm amplitude and 20-ms duration were applied at 2 Hz. Muscles were removed 10 days later.

Preparation of Muscle Fibers—Mice were killed by cervical dislocation, and interosseal muscles were removed and treated with collagenase (type I; Sigma) for 50 min at 37 °C in the presence of Tyrode solution. Single fibers were obtained by mechanically triturating muscles. For transfected muscles, fibers expressing the TRPC1 constructs were identified from the YFP fluorescence. Throughout the paper, control fibers correspond to TRPC1-YFP-negative fibers isolated from electroporated muscles except for immunolabeling experiments.

Fluorescent Immunolabeling and Confocal Microscopy—Freshly isolated fibers were plated on coated slides and slowly depolarized with a 140 K^+-containing solution before drying. Fixation and permeabilization were performed using −20 °C methanol. After fiber rehydration, the nonspecific sites were blocked with 10% normal goat serum (Sigma). Primary TRPC1 antibody (Chemicon) raised in rabbit was used and amplified with streptavidin-Cy3 (Jackson) after the use of an endogenous biotin blocking kit (avidin-biotin blocking kit, SP-2001; Vector Laboratories) to decrease background fluorescence. Fixation using paraformaldehyde led to the same expression pattern. Primary SERCA-1 antibody (Affinity Bioreagents) raised in mouse was used after the use of a kit (M.O.M. kit, BMK-2202; Vector Laboratories) for detecting mouse primary antibodies on mouse tissue. Single immunostaining of TRPC1 or SERCA-1 gave the same results as double immunostaining. Negative controls were performed in the same conditions without primary antibody and were fluorescence-free. Labeling was observed with a confocal microscope Zeiss LSM 5 and analyzed using ImageJ software. Di-8-ANEPPS (10 μM; Invitrogen) labeling was observed together with YFP fluorescence under confocal microscope.

Electrophysiology—The silicone clamp technique was used to voltage clamp or current clamp muscle fibers as described previously (12). In brief, the major part of a single fiber was electrically insulated with silicone grease so that a fiber portion (50–100 μm long) was let free of grease. A micropipette was then inserted into the fiber through the silicone layer. Under these conditions, whole cell voltage or current clamp could be achieved on the portion of the fiber free of grease. For TRPC1-YFP-positive fibers, the most fluorescent portion was left free of grease to focus measurements on the highest expressing region of the fiber. A patch clamp amplifier (Bio-Logic RK-400; Claix, France) was used in the whole cell configuration, and command voltage pulse generation and data acquisition were done using the pClamp10 software (Axon Instruments, Inc.) driving an A/D converter (Digidata 1440A; Axon Instruments, Inc.). Cell capacitance used to calculate current density was determined by integration of a current trace obtained with a 10-mV hyperpolarizing pulse from the holding potential.

Mn^{2+} Quenching Experiments and Ca^{2+} Measurements using Fura-2—Prior to experiments, cells were dialyzed for 20 min with an internal pipette solution containing 100 μM fura-2 crushed into the dish bottom to allow intracellular dialysis. Fura-2 fluorescence was measured between 520 and 560 nm. Images from a region of 20-μm diameter on the silicone-free extremity of the cell under study were captured with CCD camera at a frequency of 0.1 or 0.2 Hz. For quenching experiments, a Ca^{2+}-insensitive wavelength excitation (360 nm) was used to detect Mn^{2+} entry. The rate of Mn^{2+} influx was estimated by fitting a linear regression to the fluorescence records. For Ca^{2+} measurement, fura-2 was excited at Ca^{2+}-sensitive wavelengths (340 and 380 nm) and after background subtraction, the ratio F340/F380 was calculated to estimate intracellular $[Ca^{2+}]$. The excitation wavelengths used were different from the one used for detecting YFP fluorescence so that this latter did not interfere.

Ca^{2+} Transient Measurements Using Indo-1—After partial insulation (see above), fibers were dialyzed with an internal solution containing 200 μM indo-1. Indo-1 fluorescence was measured at 405 (F405) and 485 nm (F485) by two photomultipliers upon 360-nm excitation. To calibrate the indo-1 response and calculate $[Ca^{2+}]$, the standard ratio method was used with the parameters: r = F405/F485, with R_{min}, R_{max}, K_D, and β having their usual definitions. Results were either expressed in terms of indo-1% saturation or in actual free Ca^{2+} concentration. *In vivo* values for R_{min}, R_{max}, and β were measured using procedures described previously (13).

Solutions—For electrophysiological experiments and resting Ca^{2+} imaging, the external saline corresponded to a Tyrode solution containing 140 mM NaCl, 5 mM KCl, 2.5 mM $CaCl_2$ (or 0), 2 mM $MgCl_2$, and 10 mM HEPES adjusted to pH 7.2 with NaOH. For Ca^{2+} transient measurements, the external solution contained 140 mM triethylammonium-methanesulfonate, 2.5 mM $CaCl_2$, 2 mM $MgCl_2$, 2 μM tetrodotoxin, and 10 mM HEPES adjusted to pH 7.2 with tetraethylammonium-OH. For quenching experiments, the external solution (140 mM tetraethylammonium-containing solution for resting measurements and Tyrode for cyclopiazonic acid (CPA) experiments) was replaced by a Ca^{2+}-free and Mg^{2+}-free solution containing 3 mM $MnCl_2$. The whole cell intrapipette solution contained 120 mM potassium-glutamate, 5 mM Na_2-ATP, 5 mM Na_2-phosphocreatine, 5.5 mM $MgCl_2$, 5 mM glucose, 5 mM HEPES adjusted to pH 7.2 with potassium-OH. Fura-2 and indo-1 were dissolved in distilled water at 10 mM and CPA in dimethyl sulfoxide at 50 mM and were diluted into appropriate solutions at the required concentrations. Cells were exposed to different solutions by placing them in the mouth of a perfusion tube from which

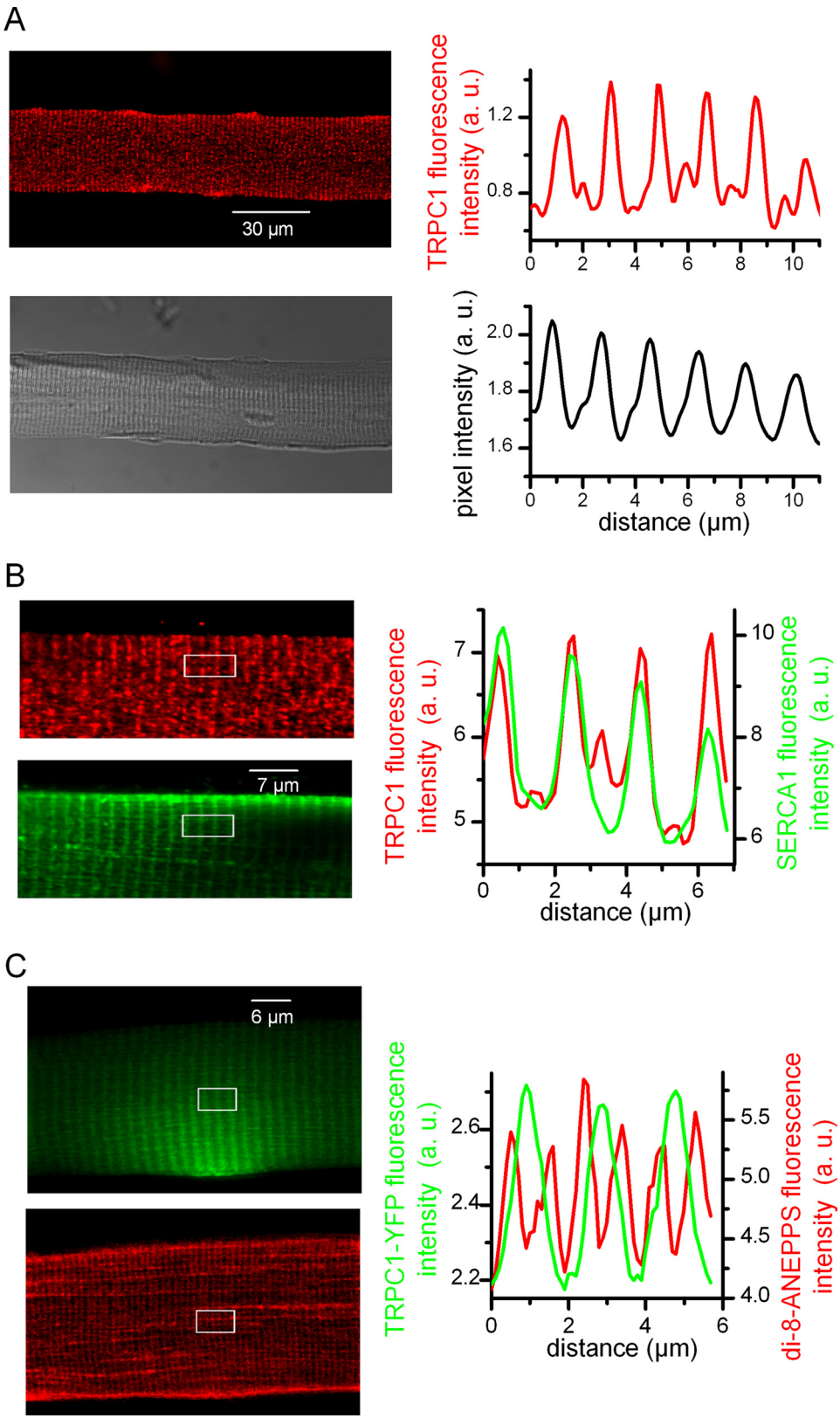

FIGURE 1. **Patterns of expression of endogenous and exogenous TRPC1.** *A*: *Left*, confocal image of immunofluorescence labeling of TRPC1 (*upper*) and corresponding transmitted light image of the fiber (*lower*). *Right*, average intensity profiles of immunofluorescence (*upper*) and transmitted light (*lower*) obtained from the same region of a fiber. *B*: *Left*, confocal images of double immunofluorescence labeling of TRPC1 (*upper*, *red*) and SERCA-1 (*lower*, *green*) in the same fiber. *Right*, average intensity profiles from the *white box region* in the next corresponding images. *C*: *Left*, confocal images of the YFP fluorescence (*green*) and of di-8-ANEPPS staining (*red*) from a TRPC1-YFP-positive fiber. *Right*, average intensity profiles from the *white box region* in the next corresponding images.

flowed by gravity the rapidly exchanged solutions. Experiments were carried out at room temperature.

Statistics—Least squares fits were performed using a Marquardt-Levenberg algorithm routine included in Microcal Origin (Microcal Software, Inc., Northampton, MA). Data are given as means ± S.E. and compared using different tests as indicated in the text. Differences were considered significant when $p < 0.05$.

RESULTS

Localization of Endogenous and Exogenous TRPC1 in Muscle Fibers—We first examined the spatial expression pattern of endogenous TRPC1 proteins in isolated muscle fibers. Confocal images of immunostaining for TRPC1 revealed an intracellular striated expression pattern perpendicular to the longitudinal axis of the fiber, whereas TRPC1 immunolabeling was absent from the sarcolemma (Fig. 1*A*). The fluorescence intensity profile showed periodic peaks of high intensity fluorescence with a mean spacing of 1.81 ± 0.02 μm in nine immunostained fibers whereas fainter fluorescence peaks could be also detected in between. The corresponding transmitted light images indicated that the frequency of the high intensity peaks of fluorescence matched the frequency of the classic repeats of the A and I bands of the sarcomeres. Co-immunostaining of muscle fibers with TRPC1 antibody and antibody against SERCA-1, the SR Ca^{2+} pump, showed that the high density expression sites of TRPC1 coincided with the labeling of SERCA-1 (Fig. 1*B*). The strong co-localization of TRPC1 with SERCA-1 demonstrates that endogenous TRPC1 mainly localized to the longitudinal SR.

We next explored the localization of exogenous TRPC1 in adult muscle fibers transfected with a TRPC1-YFP construct. YFP fluorescence could be generally observed in about 20–30 fibers isolated from the transfected muscles after collagenase treatment. Usually, expres-

sion of TRPC1-YFP was local, the most frequently at the extremity of the fibers. As observed for endogenous TRPC1, confocal images revealed an intracellular striated expression pattern of TRPC1-YFP (Fig. 1*C*). The mean spacing of high intensity YFP fluorescence was 1.88 ± 0.06 μm in six transfected cells, a value not significantly different from the mean spacing of high intensity fluorescence peaks of immunolabeled endogenous TRPC1 ($p = 0.09$ (Mann-Whitney)). Staining of the t-tubule membranes with di-8-ANEPPS in the transfected cells was observed as a double band distributed on both sides of the TRPC1-YFP fluorescence signal, indicative of TRPC1-YFP distribution at the level of the longitudinal SR as observed for the endogenous TRPC1.

Electric Properties and Mn^{2+} Influx in TRPC1-YFP-transfected Fibers—Our immunolabeling experiments indicated that TRPC1 channels localized mainly to the longitudinal SR. However, as reported above, several works have proposed that TRPC1 operates in the plasma membrane in skeletal muscle. We thus performed a series of electrophysiological experiments to investigate the possible modifications of the electric properties of muscle cells overexpressing TRPC1 (Fig. 2). Under current clamp conditions, a number of parameters were compared between control and TRPC1-YFP-positive cells, including the spike value of the first action potential (AP) and its duration at 50 and 20% of AP repolarization in a 50-Hz train, and the magnitude of the membrane depolarization at the end of an AP train. Under voltage clamp conditions, the holding current at −80 mV was measured, and the membrane conductance was estimated by applying voltage ramps, bringing the holding potential from −100 to −60 mV. Statistical analysis indicated that none of these parameters was significantly changed in TRPC1-YFP-positive cells, indicating that overexpression of TRPC1 did not alter electric sar-

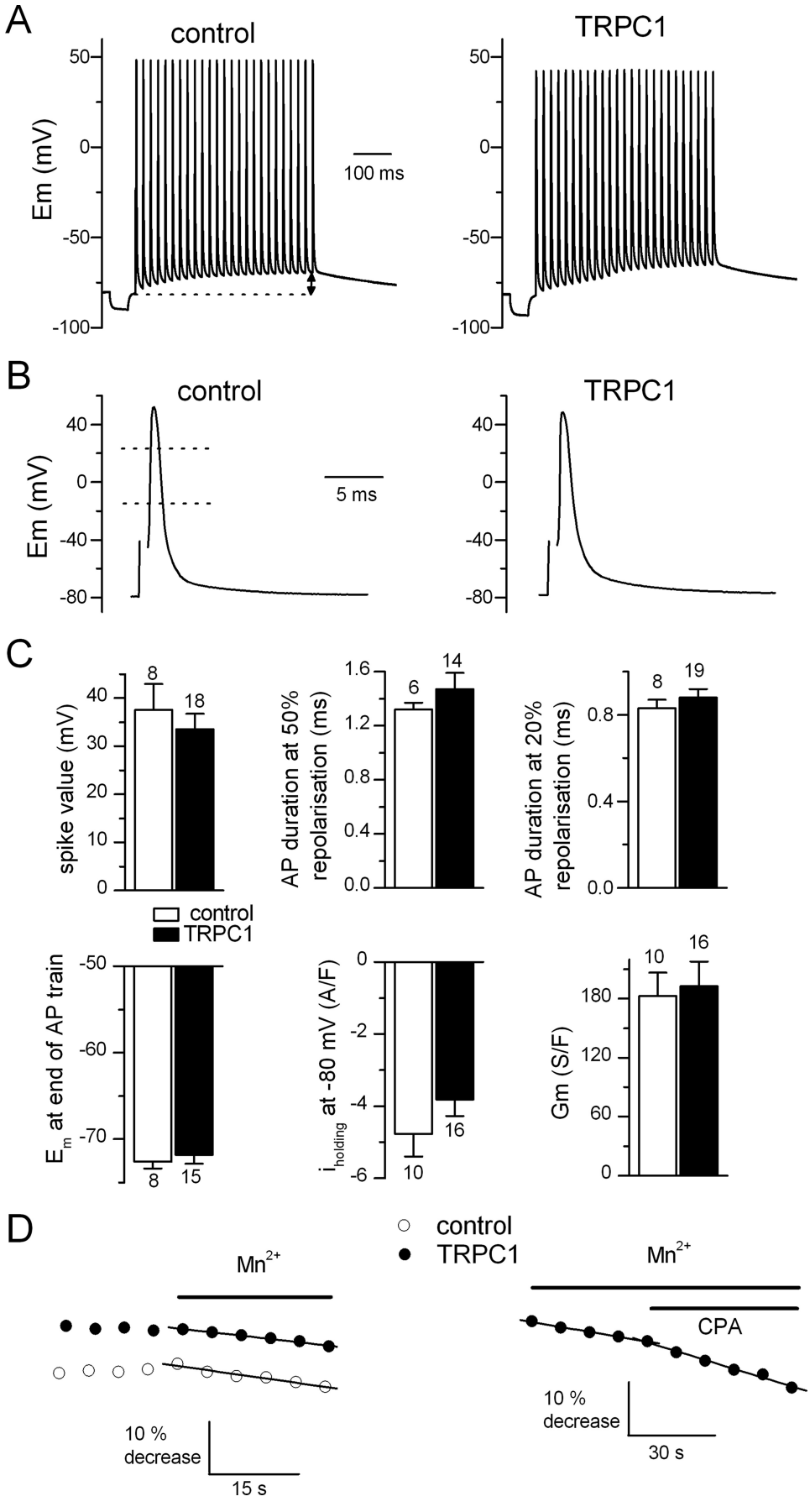

colemmal properties in resting and excited muscle cells (Fig. 2*C*). In a recent study, we demonstrated that the influx of divalent cations at rest and the influx evoked by SR depletion were both electrically silent in skeletal muscle (11). Consequently, the absence of a change in the electric properties of TRPC1-YFP-positive fibers would not exclude that the influx of divalent cations through sarcolemma could have been modified in response to overexpression of TRPC1 but not detected by electrophysiological approach. Influx of divalent cations was then monitored in control and TRPC1-YFP-positive fibers using the Mn^{2+} quenching technique, which offers a higher resolution than the measurement of currents or membrane potential changes. The *left panel* of Fig. 2*D* shows that the rate of Mn^{2+} entry was not significantly changed in resting fibers voltage clamped at −80 mV. In average, the basal rate of Mn^{2+} quenching was 9.8 ± 2.3%·min^{-1} in control ($n = 5$) and 10.5 ± 1.6%·min^{-1} in TRPC1-YFP-positive fibers ($n = 6$) ($p = 0.8$ (*t* test)). However, TRPC1-YFP-transfected fibers responded differently from the control cells to the SR Ca^{2+} ATPase inhibitor CPA (Fig. 2*D*, *right panel*). Although the rate of Mn^{2+} influx was previously reported to be slightly decreased in response to addition of CPA to the external solution under current clamp conditions (11), in contrast we observed that CPA significantly increased the rate of Mn^{2+} influx by 59 ± 19% ($p = 0.009$ (paired *t* test), $n = 10$) in TRPC1-YFP-transfected fibers under the same experimental conditions. This result can be interpreted in two ways. Either the store depletion induced by CPA in cells overexpressing TRPC1 is of the same magnitude as in control but the sarcolemmal Mn^{2+} influx is potentiated through possible sarcolemmal TRPC1 channels in higher density, or the Mn^{2+} influx is potentiated because of a deeper depletion of the SR in the TRPC1-YFP-positive muscle fibers which in turn amplifies a sarcolemmal store-operated Mn^{2+} influx through a pathway independent of TRPC1. The clear localization of endogenous and exogenous TRPC1 in the longitudinal SR prompted us to test the second hypothesis and to investigate a possible involvement of TRPC1 in the Ca^{2+} efflux from the SR.

SR Ca^{2+} Efflux in TRPC1-YFP-transfected Fibers—In this series of experiments, the change in intracellular Ca^{2+} in response to the addition of CPA was monitored in control and in TRPC1-YFP-transfected fibers under current clamp conditions. A first striking observation was that the great majority of TRPC1-YFP-transfected fibers (8 of 11 tested) exposed to CPA contracted locally at the level of the highest YFP fluorescent zone, assumed to correspond to the zone where TRPC1-YFP was expressed at the highest density, whereas control fibers never contracted after the addition of CPA during the course of experiments. This local contractile response was still evoked in TRPC1-YFP-positive fibers in the absence of external Ca^{2+} (Fig. 3*A*), suggesting that Ca^{2+} ions activating contraction came from internal stores. Measurement of the change in intracellular Ca^{2+} indicated that the Ca^{2+} increase in response to CPA occurred at a significantly higher rate in TRPC1-YFP-positive fibers (ratio/min 0.42 ± 0.14, $n = 11$) compared with control (ratio/min 0.07 ± 0.02, $n = 5$) ($p = 0.02$ (Mann-Whitney)) (Fig. 3, *B* and *E*). The resting [Ca^{2+}] was also found to be significantly higher in the TRPC1-YFP-positive fibers (ratio 0.27 ± 0.01, $n = 13$) compared with control (ratio 0.21 ± 0.01, $n = 6$) ($p = 0.002$ (*t* test)) (Fig. 3*D*). The local expression of TRPC1-YFP allowed us to compare on the same cell the [Ca^{2+}] and the change in Ca^{2+} induced by CPA at the level of a TRPC1-YFP-positive zone and at the level of a TRPC1-YFP-negative zone. As illustrated in Fig. 3*D*, the resting [Ca^{2+}] was significantly higher in the TRPC1-YFP-positive zone (ratio 0.27 ± 0.01, $n = 13$) than in the TRPC1-YFP-negative zone (ratio 0.25 ± 0.01, $n = 13$) ($p = 0.0005$ (Wilcoxon)). The rate of Ca^{2+} change induced by CPA was also significantly higher in the TRPC1-YFP-positive zone (ratio/min 0.42 ± 0.14, $n = 11$) than in the TRPC1-YFP-negative zone (ratio/min 0.28 ± 0.12, $n = 11$) ($p = 0.006$ (paired *t* test)) (Fig. 3, *C* and *E*), even in the absence of external Ca^{2+} (see inset Fig. 3*C*, *inset*). These two parameters were also found significantly higher in the TRPC1-YFP-negative zones compared with control fibers ($p = 0.003$ (*t* test), $p = 0.05$ (Mann-Whitney)) (Fig. 3, *D* and *E*).

Ca^{2+} Transients in TRPC1-YFP-transfected Fibers—Our Ca^{2+} measurements performed under resting conditions suggest that TRPC1 overexpression potentiates SR Ca^{2+} efflux. A last series of experiments was performed to investigate the possible involvement of TRPC1 in the intracellular Ca^{2+} movements occurring during muscle activity. For this purpose, we compared the depolarization-evoked Ca^{2+} transients in control and in TRPC1-YFP-transfected fibers. Cells were challenged under voltage clamp conditions by voltage pulses of increasing duration delivered from −80 mV to +10 mV in seven TRPC1-positive fibers and at least five control fibers (Fig. 4*A*). The peak amplitudes of the Ca^{2+} transients were found to be not significantly altered in the TRPC1-positive fibers (1.06 ± 0.16 μM, $n = 7$) for the shortest pulse (5 ms) compared with control (0.83 ± 0.04 μM, $n = 7$) ($p = 0.16$ (Mann-Whitney)). Because of heavy indo-1 saturation, this parameter was not compared for longer pulses. Fig. 4*A* also shows that there was a clear tendency toward a slowing of the decay phase of the Ca^{2+} transients in the TRPC1-positive fibers. However, fitting a single exponential plus constant function to the [Ca^{2+}] decline in each cell tested indicated that the time constant of decay was highly variable in TRPC1-YFP cells probably because of variability in the transfection efficiency from cells to cells. Only for

FIGURE 2. **Electric properties and divalent cation influx in TRPC1-YFP-transfected fibers.** *A*, trains of AP in a control (*left*) and in a TRPC1-YFP-positive fiber (*right*) stimulated by suprathreshold 0.5-ms current clamp pulses delivered at 50 Hz. Bursts of stimulation were preceded by a negative current pulse to measure the input resistance. *B*, first AP of a train in a control (*left*) and in a TRPC1-YFP-positive fiber (*right*). *C*, spike value corresponding to the maximal depolarization during the first AP of the train. AP duration at 50 and 20% repolarization corresponded to AP duration measured when E_m was returned to 50 and 20% of its spike value, respectively (in *B*, *left panel*, *dotted lines*). E_m at the end of the AP train corresponded to the value of E_m reached just before emission of the last AP of the train (in *A*, *left panel*, *double arrow*). $I_{holding}$ corresponded to the mean background current density under voltage clamp at −80 mV and G_m to the slope of the change in the current density in response to voltage ramps. *T bars* indicate ±S.E. *D*, effect of external Mn^{2+} under voltage clamp at −80 mV (*left*) and effect of CPA (50 μM) in presence of Mn^{2+} under current clamp (*right*) on fura-2 fluorescence in a control and a TRPC1-YFP-positive cell. *Straight lines* correspond to linear regressions fitted to the fluorescence records.

Ca^{2+} transients evoked by 200-ms duration voltage pulses, the mean time constant of decay was found significantly higher in TRPC1-YFP (94.4 ± 22.2 ms, $n = 7$) compared with control cells (41.2 ± 3.1 ms, $n = 5$) ($p = 0.03$ (Mann-Whitney)) (Fig. 4*B*). Finally, the resting [Ca^{2+}] was found to be not significantly different in TRPC1-positive (52.3 ± 7.2 nM) compared with control fibers (50.1 ± 9.5 nM) ($p = 0.86$ (t test)) in this series of experiments.

DISCUSSION

Our data first indicate that TRPC1 localizes to the longitudinal SR in adult mammalian skeletal muscle. Immunolabeling of endogenous TRPC1 clearly showed an intracellular striated pattern of expression and co-localization with SERCA-1, indicative of the presence of the channel in the longitudinal SR at the level of the Z discs. The faint staining for TRPC1 at the level of the M band (small intensity fluorescence peaks in between high intensity fluorescence peaks) may result from a much lower density of longitudinal SR in the region of M bands compared with the region of Z discs as recently postulated in myotubes (14). The immunolocalization of endogenous TRPC1 to the longitudinal SR was confirmed by the striated pattern of expression of the exogenous TRPC1-YFP which displayed comparable periodicity. T tubules staining with di-8-ANEPPS indicated that TRPC1-YFP distributed between two tubules surrounding Z discs also certainly because of the higher density of the longitudinal SR in this region. To our surprise, confocal microscopy images of endogenous immunostained TRPC1 as well as exogenous YFP-labeled TRPC1 never revealed any labeling compatible with a sarcolemmal localization, yet described in previous immunolabeling studies performed on adult mouse muscle fibers. However, in two of these studies, immunostaining was processed on muscle cryosections (7, 8) whereas Vande-

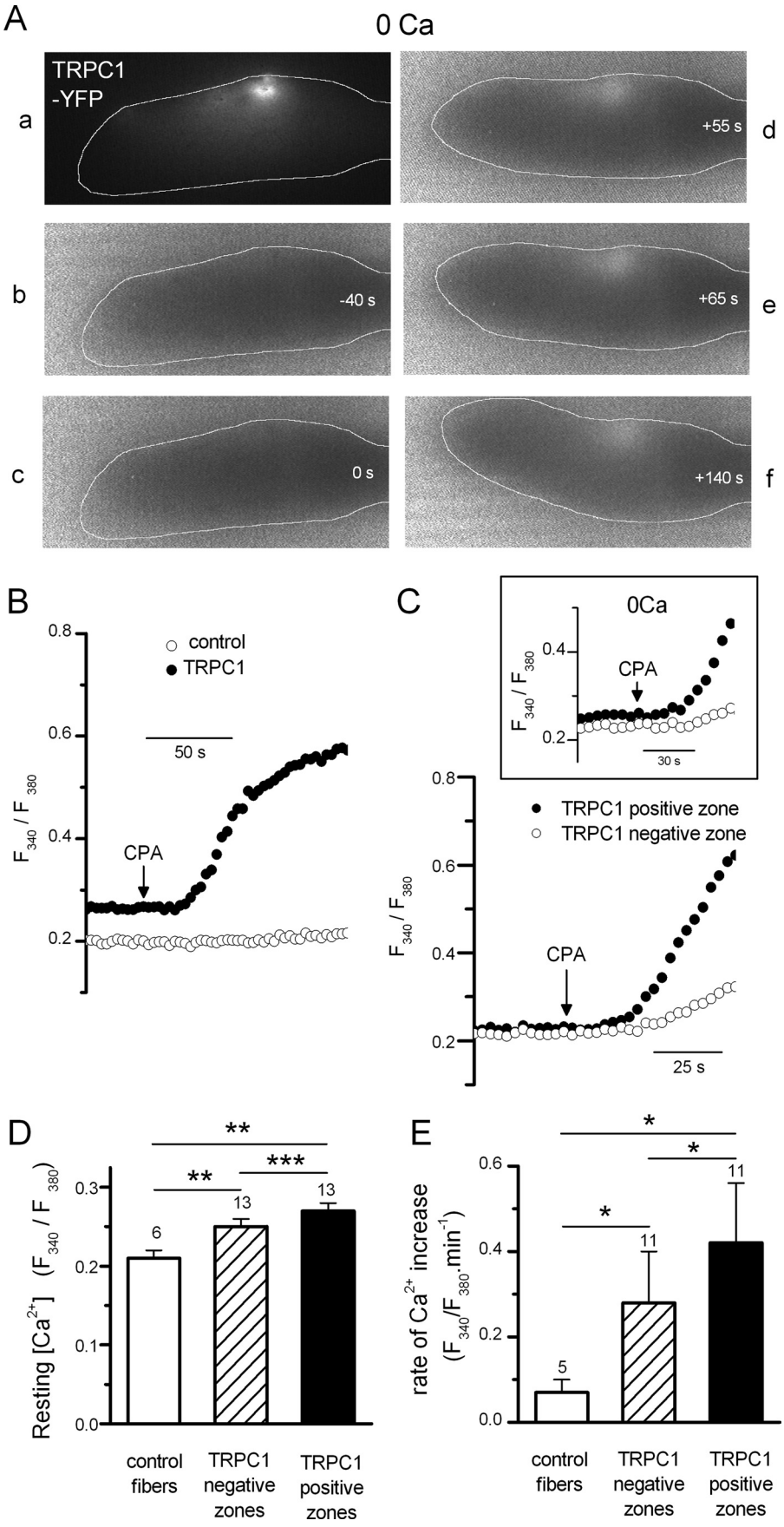

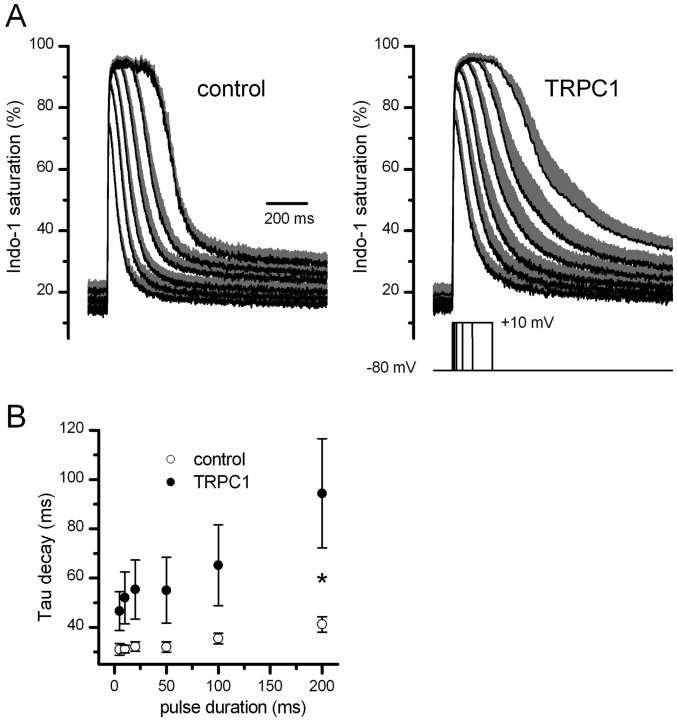

FIGURE 4. **Voltage-induced Ca^{2+} signals in TRPC1-YFP-transfected fibers.** *A*, mean (*black*) and S.E. (*gray*) of indo-1 saturation signals in response to depolarization of 5-, 10-, 20-, 50-, 100-, and 200-ms duration to +10 mV in control (*left*) and in TRPC1-YFP-positive fibers (*right*). *B*, mean values of time constant of [Ca^{2+}] decay after the end of the pulse. Values were obtained from individual exponential fits to the decay phase of the [Ca^{2+}] transients. *, $p < 0.05$.

brouck *et al.* (4) observed immunostained *mdx* muscle fibers maintained in culture using conventional microscopy. In addition, in the work of Stiber *et al.* (8), immunostaining for TRPC1 revealed a striated pattern of expression comparable with what we observed in the present study but interpreted as costamere localization because of the higher intensity of the fluorescence signal detected at the periphery of the fiber using conventional microscopy. The different experimental procedures employed in these different works might explain the different results obtained and/or interpretations given. Besides, it is plausible that the scaffolding proteins that have been shown to interact with TRPC1 are still able to interact with TRPC1 anchored in the SR membrane. Very recently, TRPC1 was also found to localize in the endoplasmic reticulum in freshly isolated adrenal medullary cells, and this distribution was confirmed by the finding that exogenous expression of TRPC1-GFP proteins in adrenal medullary cell line resulted in the localization of the fusion protein in the endoplasmic reticulum and not in the plasma membrane (15). As described in these glandular cells, the similar expression patterns we observed for endogenous and exogenous TRPC1 using two different modalities for detection give strong evidence that TRPC1 localizes to the longitudinal SR and not to the plasma membrane in adult skeletal muscle. The absence of a change in the resting electric properties and in AP in fibers overexpressing TRPC1 again argued against a possible activity of the channel at the level of the sarcolemma. The resting influx of divalent cations monitored with the Mn^{2+} quenching method was also found not to be changed in fibers overexpressing TRPC1, discarding any involvement of TRPC1 in Ca^{2+} entry at rest.

Our intracellular Ca^{2+} measurements revealed that TRPC1 is involved in the efflux of Ca^{2+} from internal stores. By inhibiting SR Ca^{2+} ATPases, CPA indeed produced a progressive increase in cytosolic Ca^{2+} whose mean kinetics was six times faster in fibers overexpressing TRPC1 compared with control fibers. When measured on the same fiber, this kinetics was in average 1.9 ± 0.38 times faster at the level of the TRPC1-positive area compared with the TRPC1-negative area. The fact that the Ca^{2+} rise produced in response to CPA poisoning occurred in the absence of external Ca^{2+} gave evidence that the more pronounced cytosolic Ca^{2+} increase in fibers overexpressing TRPC1 resulted from a potentiated SR Ca^{2+} leak. The local contractile response frequently observed at the level of the TRPC1-overexpressing areas and never observed in control fibers was another proof of the elevated Ca^{2+} leak at the level of the TRPC1-overexpressing areas. In the absence of CPA, a significant higher resting [Ca^{2+}] at the level of the overexpressing zone also attested to the potentiated Ca^{2+} leak that exogenous TRPC1 channels were likely responsible for. Finally, it is likely that the increase in the Mn^{2+} quenching rate produced by CPA poisoning in fibers overexpressing TRPC1 but not in control fibers resulted from the deeper SR depletion, which in turn activated a store-operated sarcolemmal divalent cation entry. Taken together, these data demonstrate that TRPC1 channels operate as Ca^{2+} leak channels in the longitudinal SR of skeletal muscle.

Despite the sizeable increase in SR Ca^{2+} efflux induced by TRPC1 overexpression, the Ca^{2+} transients evoked by depolarization were not markedly altered in fibers overexpressing TRPC1. However, in contrast to CPA experiments that made use of a Ca^{2+} imaging system that allowed accura surrounding of the overexpression area, the voltage-evoked changes in intracellular Ca^{2+} were measured on a voltage-clamped cell portion that extended beyond the restricted zone of overexpression so that possible modifications of Ca^{2+} transients at the level of this area could be lost in the whole signal. Additionally, the use of the less sensitive dye indo-1 may explain that a difference in the

FIGURE 3. **Effect of CPA on intracellular [Ca^{2+}] in TRPC1-YFP-transfected fibers.** *A*, local contractile response evoked by addition of CPA in a TRPC1-YFP-positive fiber set to −80 mV in current clamp and bathed in a Ca^{2+}-free solution. *Panel a* shows the YFP fluorescence of the voltage clamped portion of the fiber. *Panels b–f* show fura-2 fluorescence ratio changes at different times (*white numbers*) before and after addition of CPA. Note the local increase in ratio at the level of the YFP-labeled area. The fiber has been outlined to better distinguish changes in cell shape induced by local contractile response. *B*, changes in fura-2 fluorescence ratio induced by addition of CPA in a control and in a TRPC1-YFP-positive fiber. *C*, changes in fura-2 fluorescence ratio induced by CPA at the level of the TRPC1-YFP-negative and TRPC1-YFP-positive zones in a TRPC1-YFP-positive fiber bathed in a normal external solution (*right*) and in another positive fiber bathed in Ca^{2+}-free solution (*inset*). Membrane potential was set to −80 mV under current clamp. *D*, histograms showing the mean resting values of fura-2 fluorescence at −80 mV in control fibers and at the level of TRPC1-YFP-negative and TRPC1-YFP-positive zones in TRPC1-YFP-positive fibers. *E*, histograms comparing the mean rate of intracellular [Ca^{2+}] change induced by CPA (estimated by fitting fluorescence increase with linear regression) in control fibers and at the level of TRPC1-YFP-negative and TRPC1-YFP-positive zones in TRPC1-YFP-positive fibers. *, $p < 0.05$; **, $p < 0.005$; and ***, $p < 0.0005$. *T bars* indicate ±S.E.

resting Ca^{2+} could not be found again between control and TRPC1-overexpressing fibers in this series of experiments. Nevertheless, for the longest depolarization pulses applied, the time constant decay of Ca^{2+} transients was found to be significantly higher in fibers overexpressing TRPC1 whereas a tendency toward a slower Ca^{2+} transient decay was observed for shorter pulses. This result indicates, at least for the longest pulses, that the potentiated SR Ca^{2+} efflux through overexpressed TRPC1 was high enough to slow the Ca^{2+} removal process exerted by the SR Ca^{2+} pumps during the Ca^{2+} transient relaxing phase.

Up until now, Ca^{2+} leak through the SR membrane has been considered to occur mainly through the ryanodine receptor in skeletal muscle. Another channel belonging to the TRP family, the vanilloid receptor subtype 1 (TRPV1), has also been found to localize to the SR and to leak Ca^{2+} under resting conditions (16). Together with the ryanodine receptor and TRPV1, TRPC1 may thus operate as a parallel passive leakage pathway in balance with SERCA to set the resting Ca^{2+}. This result has considerable physiopathological significance. Numbers of studies suggest that TRPC1 is involved in the store-operated Ca^{2+} entry, but, to our knowledge, there is no direct evidence that TRPC1 channels correspond to the sarcolemmal Ca^{2+} influx pathway in skeletal muscle. We propose that TRPC1 is indeed implicated in the store-operated Ca^{2+} influx but operates upstream by contributing to SR Ca^{2+} efflux and SR depletion as suggested by our Mn^{2+} quenching experiments. In a pathological point of view, it was reported that the expression level of TRPC1 was increased in skeletal muscle from *mdx* mice (7). The augmented SR Ca^{2+} leak through TRPC1 channels may contribute to the chronic elevation of resting cytosolic Ca^{2+} that, although still debated, has been described in dystrophic muscle (for review, see Ref. 17). In parallel, as suggested by our data obtained on Ca^{2+} transients in TRPC1-overexpressing fibers, the exacerbated Ca^{2+} leak through TRPC1 channels may also account for the slowing of the decay phase of the Ca^{2+} transient that has been reported in dystrophic muscle by several studies (13, 18, 19).

In conclusion, our study gives evidence for the presence of the TRPC1 channel in the membrane of the longitudinal SR where it operates as a Ca^{2+} leak channel. TRPC1 is thence deeply involved in intracellular Ca^{2+} homeostasis at rest and during muscle activation by potentially regulating SR Ca^{2+} content, resting cytosolic Ca^{2+} and kinetics of the voltage-evoked Ca^{2+} transients.

Acknowledgments—We thank Sandrine Pouvreau for help in confocal microscope observations and Vincent Jacquemond and Maelle Jospin for critical comments on the manuscript.

REFERENCES

1. Venkatachalam, K., and Montell, C. (2007) *Annu. Rev. Biochem.* **76,** 387–417
2. Birnbaumer, L. (2009) *Annu. Rev. Pharmacol. Toxicol.* **49,** 395–426
3. Rychkov, G., and Barritt, G. J. (2007) *Handb. Exp. Pharmacol.* **179,** 23–52
4. Vandebrouck, C., Martin, D., Colson-Van Schoor, M., Debaix, H., and Gailly, P. (2002) *J. Cell Biol.* **158,** 1089–1096
5. Louis, M., Zanou, N., Van Schoor, M., and Gailly, P. (2008) *J. Cell Sci.* **121,** 3951–3959
6. Formigli, L., Sassoli, C., Squecco, R., Bini, F., Martinesi, M., Chellini, F., Luciani, G., Sbrana, F., Zecchi-Orlandini, S., Francini, F., and Meacci, E. (2009) *J. Cell Sci.* **122,** 1322–1333
7. Gervásio, O. L., Whitehead, N. P., Yeung, E. W., Phillips, W. D., and Allen, D. G. (2008) *J. Cell Sci.* **121,** 2246–2255
8. Stiber, J. A., Zhang, Z. S., Burch, J., Eu, J. P., Zhang, S., Truskey, G. A., Seth, M., Yamaguchi, N., Meissner, G., Shah, R., Worley, P. F., Williams, R. S., and Rosenberg, P. B. (2008) *Mol. Cell. Biol.* **28,** 2637–2647
9. Vandebrouck, A., Sabourin, J., Rivet, J., Balghi, H., Sebille, S., Kitzis, A., Raymond, G., Cognard, C., Bourmeyster, N., and Constantin, B. (2007) *FASEB J.* **21,** 608–617
10. Allard, B., Couchoux, H., Pouvreau, S., and Jacquemond, V. (2006) *J. Physiol.* **575,** 69–81
11. Berbey, C., and Allard, B. (2009) *Biophys. J.* **96,** 2648–2657
12. Pouvreau, S., Collet, C., Allard, B., and Jacquemond, V. (2007) *Methods Mol. Biol.* **403,** 185–194
13. Collet, C., Allard, B., Tourneur, Y., and Jacquemond, V. (1999) *J. Physiol.* **520,** 417–429
14. Cusimano, V., Pampinella, F., Giacomello, E., and Sorrentino, V. (2009) *Proc. Natl. Acad. Sci. U.S.A.* **106,** 4695–4700
15. Matsuoka, H., Harada, K., Ikeda, T., Uetsuki, K., Sata, T., Warashina, A., and Inoue, M. (2009) *Am. J. Physiol. Cell Physiol.* **296,** C889–C899
16. Xin, H., Tanaka, H., Yamaguchi, M., Takemori, S., Nakamura, A., and Kohama, K. (2005) *Biochem. Biophys. Res. Commun.* **332,** 756–762
17. Gailly, P. (2002) *Biochim. Biophys. Acta* **1600,** 38–44
18. Turner, P. R., Westwood, T., Regen, C. M., and Steinhardt, R. A. (1988) *Nature* **335,** 735–738
19. Woods, C. E., Novo, D., DiFranco, M., and Vergara, J. L. (2004) *J. Physiol.* **557,** 59–75